CONEM2014
VIII CONGRESSO NACIONAL DE ENGENHARIA MECÂNICA
UBERLÂNDIA - MG - BRASIL 10 A 15 DE AGOSTO DE 2014

FINITE ELEMENT ANALYSIS OF PRESSURE-DRIVEN LAMINAR FLOW INSIDE PERIODICALLY STAGGERED ARRAYS

Gustavo Charles P. de Oliveira, gustavo.oliveira@uerj.br[1]
Gustavo Anjos, gustavo.anjos@uerj.br[1]
José Pontes, jopontes@metalmat.ufrj.br[2]
Norberto Mangiavacchi, norberto@uerj.br[1]
[1]Group of Environmental Studies for Water Reservoirs - GESAR, State University or Rio de Janeiro, Rua Fonseca Teles, 121, 20940-903, São Cristóvão, Rio de Janeiro, RJ, Brazil.
[2]Metallurgy and Materials Engineering Department, Federal University of Rio de Janeiro, PO Box 68505, 21941-972 Rio de Janeiro, RJ, Brazil

Abstract: *This work applies a finite element method (FEM) approach with periodic boundary conditions to the Navier-Stokes equations for an incompressible fluid moving inside a planar hexagonally-arranged domain. We highlight the usability of a model which decomposes the total pressure into a linear part and a periodic component to ensure the maintenance of mass flow across the domain. Besides, we apply a strategy to eliminate degrees of freedom directly inside the global matrix, so enforcing the periodicity for Dirichlet and Neumann conditions accordingly. Numerical simulations under low Reynolds number are presented for staggered and nonstaggered array configurations. Additionally, the periodic implementation is verified in contrast to the classical analytical solution of a Taylor vortex, thus providing good representation of the flow desired.*
Keywords: *FEM, periodic boundary conditions, incompressible fluid, staggered cylinder.*

1. INTRODUCTION

Patterns interspersed in the manner of periodic arrays can be viewed as unit cells which replicate spatially along a domain. In engineering applications, examples of such arrangements extend across packed bed reactors (Lahbabi and Chang, 1986), electromagnetic fields (McGrath and Pyati, 1996), heat exchangers (Beale, 2007), up to composite micromechanical models (Tyrus *et al.*, 2007). Notwithstanding, in the field of the fluid dynamics, the investigation of hydrodynamic properties of periodic fluid flows has also been envisaged with different models and methods.

For fluid applications, motivational aspects concerning periodic arrays come up with configurations at which the fluid motion around obstacles is the main subject of the investigations, such as arrangement of staggered cylinders, bundle of tube banks (Segal *et al.*, 1994), and serrated channels (Murthy and Mathur, 1997). In general, due to properties of symmetry or uniformity, three-dimensional problems can be reduced to two-dimensional models without losing their validity. More recently, works related not only to fibrous media (Yazdchi *et al.*, 2011), but also to complex pore-scale media (Zenklusen *et al.*, 2014) have proposed periodic arrays already well known, but modified in complexity to suit to certain physical conditions.

This work applies a finite element method (FEM) approach with periodic boundary conditions to the Navier-Stokes equations for an incompressible fluid moving inside a hexagonally-arranged domain, where the keypoint is to build a robust numerical code capable to handle fluid flows under periodic conditions. In order to verify the authenticity of the results, numerical tests are performed against a classic solution of a starting Taylor vortex flow, so settling a fair benchmark. Moreover, we use adaptive meshes to bring up good capture of boundary layers developing around edges.

The paper is organized in the following structure: Section 2 describes the mathematical formulation considering the model of periodic pressure; Section 3 addresses a methodology to impose periodicity on a finite element mesh by overloading degrees of freedom; Section 4 presents some numerical simulations. Finally, brief conclusions are drawn.

2. MATHEMATICAL FORMULATION

This section describes the domain as well as the governing equations for the problem intended herein. Consider $\Omega \in \mathbb{R}^2$ a convex set with boundary Γ such that the latter is sectioned by a union of partial boundaries as depicted in Fig. 1. Γ_L and Γ_R are identified by points spaced uniformly at left and right of the domain to explicit the periodic part of the boundary, both being defined, respectively, as the master portion and the slave portion of the unit cell. Similarly, Γ_B and Γ_T are the lower and upper bounds, while the four numbered corner arcs form the remnant part of the outer boundary. To keep the conformity of the arrangement, Γ_C is placed as a central obstacle inside the domain making up a complete circle

of radius r. In turn, the flow passageway amidst staggered-like shapes of tube banks (cylinders arranged perpendicularly) can be studied by keeping or removing Γ_C, in staggered and nonstaggered fashions. For better identification, the thicker borders outside the periodic portions are to indicate no-slip conditions, while the thinner ones to denote slip conditions.

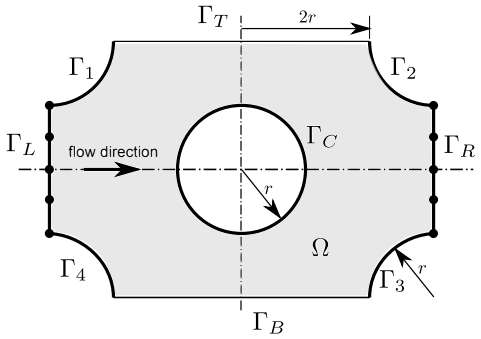

Figure 1: Two-dimensional model of a hexagonal periodic array for staggered tubes (Yazdchi *et al.*, 2011).

The flow is driven from left to right by the imposition of a constant pressure gradient and forced to reenter into the domain after leaving the periodic extremum downstream. Following the model by Patankar *et al.* (1977) for laminar flow in fully developed regime, we decompose the total pressure into a linear part plus a periodic parcel as

$$p(\mathbf{x},t) = -\beta(\mathbf{x}\cdot\hat{\mathbf{i}}) + P(\mathbf{x},t), \tag{1}$$

where β is the value of the constant pressure gradient, which decays along the streamwise direction given by the unitary vector $\hat{\mathbf{i}}$, and $P(\mathbf{x},t)$ is the periodic component. As usually defined, $\mathbf{x}\in\mathbb{R}^2$, while t is the time. However, to treat the problem in terms of dimensionless quantities, β should be rewritten as

$$\beta = \frac{\rho_0 U_0^2 \beta^*}{L_0}, \tag{2}$$

where ρ_0, U_0, L_0 are reference values for density, velocity, and length, respectively, so that β^* renders a dimensionless quantity fostering a certain mass flow (Lahbabi and Chang, 1986), (Murthy and Mathur, 1997).

The movement of the fluid is governed by the dimensionless incompressible Navier-Stokes equations imbued with the pressure periodic and free of gravitational effects. After replacing the original pressure term in the Navier-Stokes equations with the Eq. 1, applying the gradient operator, and organizing the terms, the model can be written as

$$\frac{D\mathbf{u}}{Dt} = \beta\hat{\mathbf{i}} - \nabla P + \frac{1}{Re}\nabla\cdot\left[\mu(\nabla\mathbf{u} + \nabla\mathbf{u}^T)\right] \tag{3}$$

$$\nabla\cdot\mathbf{u} = 0 \tag{4}$$

with

$$\frac{D\mathbf{u}}{Dt} = \frac{\partial\mathbf{u}}{\partial t} + \mathbf{u}\cdot\nabla\mathbf{u}\,. \tag{5}$$

Above, the quantities now appearing are the velocity field $\mathbf{u}$, the viscosity μ, and the Reynolds number Re. For clarity, the "$*$" was dropped out of β, as well as the steps to get dimensionless terms omitted.

With these symmetry and periodic boundary conditions well defined, the mathematical model seeks the solution $(\mathbf{u}, P)\times t$ subject to the initial condition

$$\mathbf{u}(\mathbf{x},0) = 0, \quad \text{for} \quad \mathbf{x}\in\Omega \tag{6}$$

and

$$\mathbf{u}|_{\Gamma_C} = \mathbf{u}|_{\Gamma_j} = \mathbf{0}, \quad \text{for} \quad (0,\tau], \quad j = 1,2,3,4 \tag{7}$$

$$\mathbf{u}\cdot\mathbf{n}|_{\Gamma_T} = \mathbf{u}\cdot\mathbf{n}|_{\Gamma_B} = 0, \quad \text{for} \quad (0,\tau] \tag{8}$$

$$\mathbf{u}|_{\Gamma_L} = \mathbf{u}|_{\Gamma_R}, \quad \text{for} \quad (0,\tau] \tag{9}$$

$$\left.\frac{\partial\mathbf{u}}{\partial\mathbf{n}}\right|_{\Gamma_L} = -\left.\frac{\partial\mathbf{u}}{\partial\mathbf{n}}\right|_{\Gamma_R}, \quad \text{for} \quad (0,\tau] \tag{10}$$

$$P|_{\Gamma_L} = P|_{\Gamma_R} \quad \text{for} \quad (0,t] \tag{11}$$

$$\left.\frac{\partial P}{\partial\mathbf{n}}\right|_{\Gamma_L} = -\left.\frac{\partial P}{\partial\mathbf{n}}\right|_{\Gamma_R}, \quad \text{for} \quad (0,\tau] \tag{12}$$

$$P(\mathbf{x}_B,t) = 0, \quad \text{at} \quad \mathbf{x}_B\in\Gamma_B, \text{for} \quad (0,\tau]. \tag{13}$$

3. IMPLEMENTATION OF PERIODIC BOUNDARY CONDITIONS

In order to implement PBC, the meshes need to be designed to guarantee the correct spatial correspondence between the nodes belonging to the periodic boundaries Γ_L and Γ_R. Firstly, we seek satisfy the relation

$$(\mathbf{x}_L;\gamma) := \{\mathbf{x}_{L,1}, \mathbf{x}_{L,2}, \ldots, \mathbf{x}_{L,\gamma}\}$$
$$(\mathbf{x}_R;\gamma) := \{\mathbf{x}_{R,1}, \mathbf{x}_{R,2}, \ldots, \mathbf{x}_{R,\gamma}\},$$

by defining the geometrical periodicity of the mesh if $y_L = y_R$, for γ nodes distributed evenly over the y-axis. Such correspondence is depicted in Fig. 2 by Mangiavacchi *et al.* (2013), with $\Omega_{L,1}$ and $\Omega_{R,1}$ being the 1-ring neighbour elements of Γ_L and Γ_R, respectively.

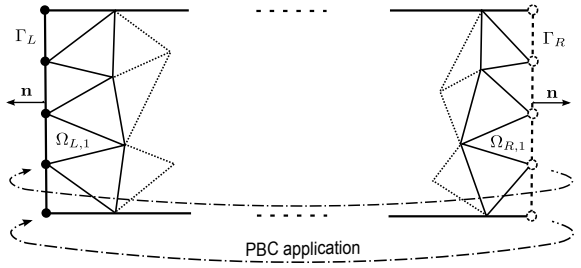

Figure 2: Geometrical sketch of the PBC implementation for a finite element mesh in two dimensions.

The incorporation of the degrees of freedom belonging to the periodic nodes is reached through a pseudounion of the shape functions of the 1-ring neighbour elements of Γ_L, Γ_R. In this way, the interelement connection is slightly changed in the global matrix of the linear system obtained after discretization, since the contributions coming from the slave nodes, stored previously in their respective rows and columns, is added to those of the master nodes. In turn, they can be eliminated safely, thus reducing the number of unknowns to be found. In reality, when joining the shape functions, we are enforcing that the Dirichlet and Neumann conditions are automatically satisfied. Explanation in details of this procedure is given in versatile ways in Sukumar and Pask (2009), Segal *et al.* (1994), and Nonino and Comini (1998). However, a brief idea is exposed as follows.

Supposing that ϕ_i is the piecewise linear shape function associated to the node $i = 1, n$ of the mesh depicted in Fig. 3, the unidimensional version of the periodicity is given by enforcing

$$\phi_1 = \phi_n. \tag{14}$$

In other words, by assuming that the derivation of the variational form of FEM is known, each integral weighted forming the matrices of the formulation suffers a slight modification at the nodes over any two elements Ω_L^e, Ω_R^e belonging apart to Γ_L and Γ_R. Different approaches are known to identify the indices of the nodes that should be periodic, either during the assembling process or by direct elimination in the global matrix of the system. By observing the Fig. 3, the periodicty

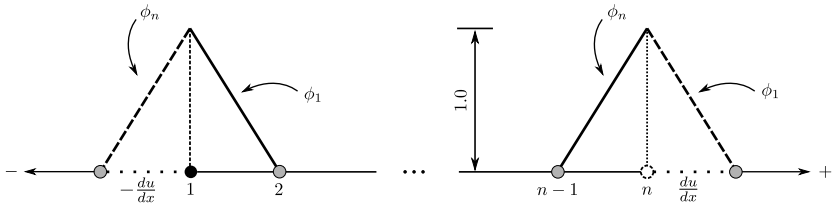

Figure 3: Unidimensional mesh of finite elements highlighting the connection of piecewise linear shape functions for a periodic domain.

occurs when joining the "dummy" left support of ϕ_1 to ϕ_n and, inversely, the right pseudosupport of ϕ_n to ϕ_1. Quite generally, we would have, in the sense of Galerkin weighting and index notation, that,

$$\int_{\Omega_L^e} \phi_i \phi_j \, dx = \left(\int_{\Omega_L^e} \phi_1 \phi_j \, dx \right) + \int_{\Omega_L^e} \phi_2 \phi_j \, dx \tag{15}$$

$$\int_{\Omega_R^e} \phi_i \phi_j \, dx = \left(\int_{\Omega_R^e} \phi_n \phi_j \, dx \right) + \int_{\Omega_R^e} \phi_{n-1} \phi_j \, dx \tag{16}$$

Inasmuch as Eq. 14 is enforced, the two integrals inside parentheses in the expressions above contribute equally for the periodic elements, thus provoking an artificial link between them, although their spatial location keep intact. Furthermore, since the normal fluxes along the x-axis can be described with -1 and +1 signs accordingly Reddy (1993), one verifies that

the Neumann condition like that declared in Eq. 10 for the periodic unidimensional case is naturally satisfied and that the fluxes stemming from the variational formulation, in reality, must be opposed one to another, i.e.,

$$(+1)\frac{\phi_n}{dx} = -(-1)\frac{\phi_1}{dx} \tag{17}$$

holds for each periodic node. The same occurs for each scalar function in the Navier-Stokes equations, namely, all the velocity components and the pressure field. For higher dimensions, the geometrical concept is that one of having the same direction of the velocity field in the exit/entrance of the periodic loop.

4. NUMERICAL SIMULATIONS AND DISCUSSION

4.1 Staggered and nonstaggered configurations

Numerical simulations carried out for both staggered and nonstaggered arrangements of the hexagonal geometry previously presented in this section. For the latter case, the central boundary Γ_C is removed. Figure 4 gives an overview of the adaptive meshes used in each problem. To capture the boundary layers forming around the corner arcs, the law of adaptiveness took into account tangential and normal variations of element sizes.

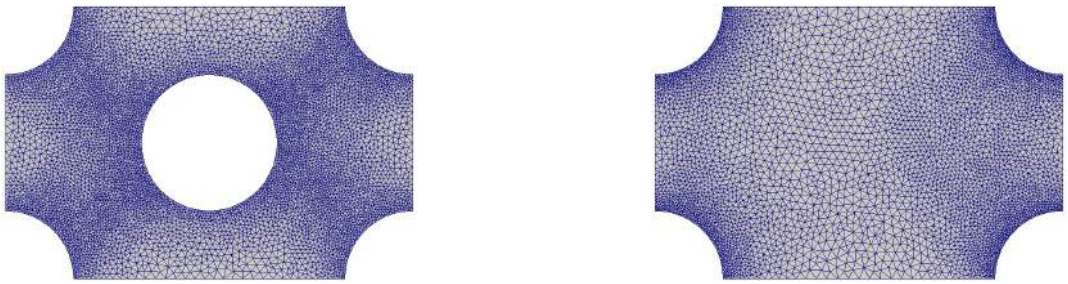

(a) (b)

Figure 4: Adaptive meshes used to simulate the periodic arrays: (a) staggered and (b) nonstaggered cases.

For all the cases of the staggered and nonstaggered simulations presented below, we consider $Re = 50$, $\beta = \frac{12}{Re}$, and $CFL = 0.5$. Figures 5, 6, and 7 depicts the velocity and periodic pressure fields for the staggered geometry at the time steps $t = 30, 80, 120$.

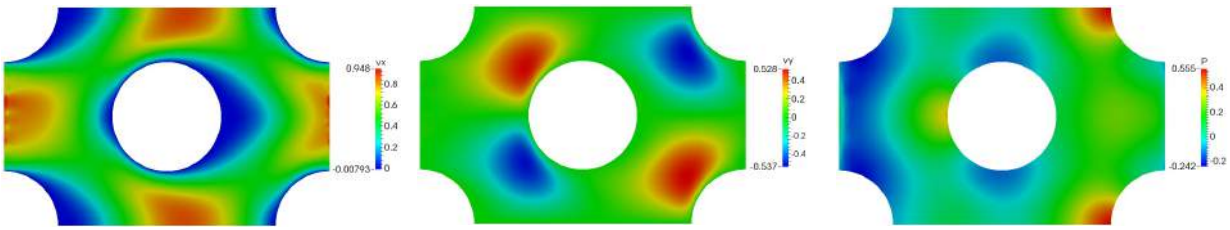

(a) (b) (c)

Figure 5: Data plotting for staggered mesh at iteration $t = 30$: (a) x-velocity; (b) y-velocity; (c) periodic pressure.

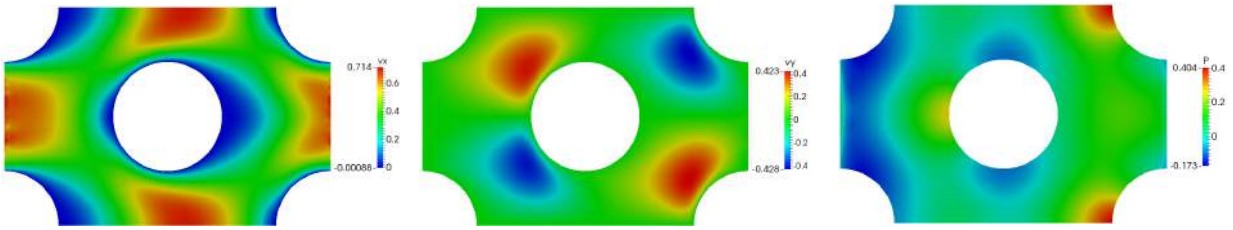

(a) (b) (c)

Figure 6: Data plotting for staggered mesh at iteration $t = 80$: (a) x-velocity; (b) y-velocity; (c) periodic pressure.

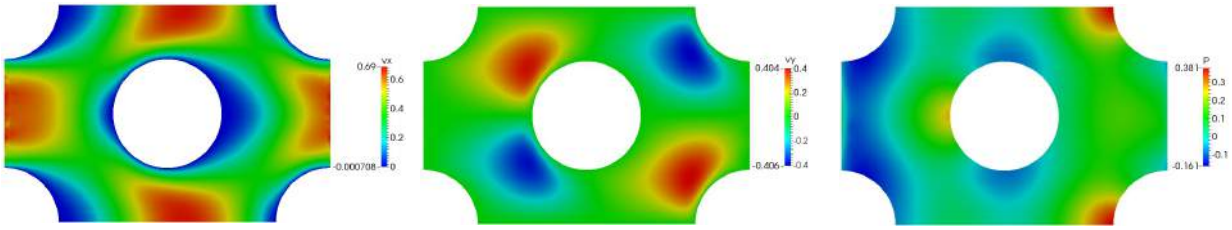

(a) (b) (c)

Figure 7: Data plotting for staggered mesh at iteration $t = 120$: (a) x-velocity; (b) y-velocity; (c) periodic pressure.

Comparatively, Figs. 8, 9, and 10 depicts the velocity and periodic pressure fields for the nonstaggered geometry at the same time steps $t = 30, 80, 120$.

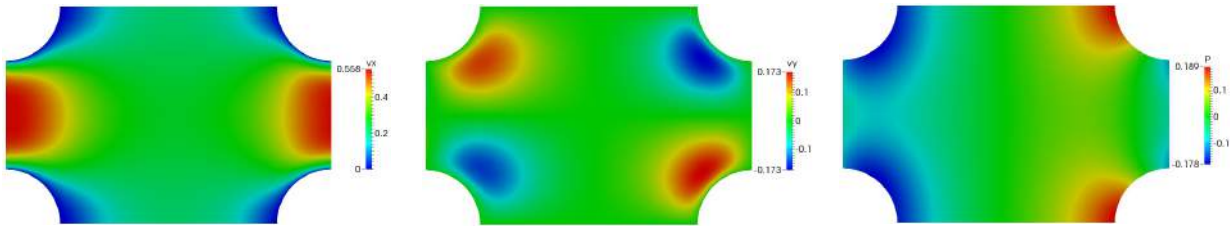

(a) (b) (c)

Figure 8: Data plotting for staggered mesh at iteration $t = 30$: (a) x-velocity; (b) y-velocity; (c) periodic pressure.

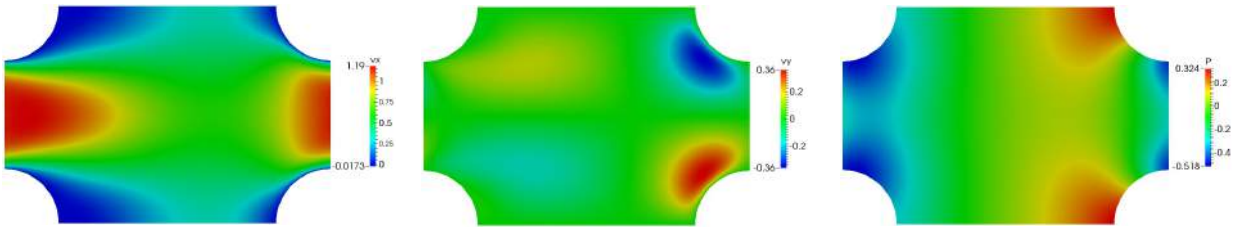

(a) (b) (c)

Figure 9: Data plotting for staggered mesh at iteration $t = 80$: (a) x-velocity; (b) y-velocity; (c) periodic pressure.

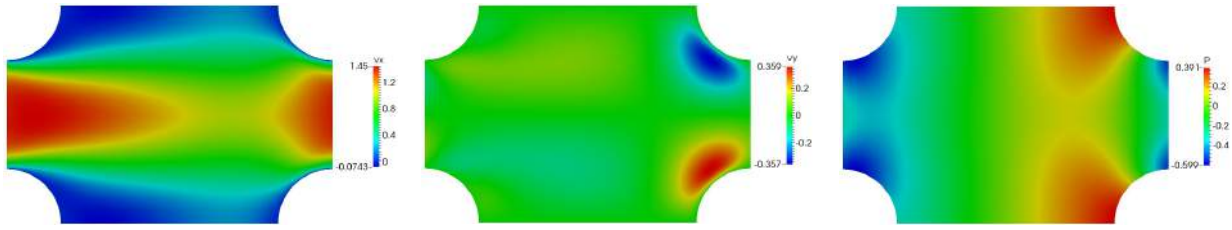

(a) (b) (c)

Figure 10: Data plotting for staggered mesh at iteration $t = 120$: (a) x-velocity; (b) y-velocity; (c) periodic pressure.

4.2 Taylor vortex

As a benchmark for code verification, the analytical solution of a Taylor vortex (see Taylor (1923)) was used to check if the periodic transition from the right boundary to the left one would introduce deformities in the solution, such as continuity and numerical dissipation issues. The transient velocity field in cylindrical coordinates is known to be

$$v_r(t) = c_1 r t^{-2} \exp\left(\frac{r^2}{4\nu t}\right), \tag{18}$$

where c_1 is a constant proportional to the circulation. Figures 11 and 12 display the velocity field of the Taylor vortex under forced convection traversing the right wall. In this case, $c_1 = 1.0$, $Re = 2000$, and a unitary streamwise velocity was added to the entire mesh nodes. As can be seen from the three snapshots, both velocity components preserve the continuity during the crossing, thus ensuring a good representation of the periodicity desired.

(a) (b) (c)

Figure 11: Streamwise velocity plotting of the Taylor vortex flow inside a channel under forced convection.

(a) (b) (c)

Figure 12: Transverse velocity plotting of the Taylor vortex flow inside a channel under forced convection.

5. CONCLUSION

This work investigated the capability of a FE code to carry out numerical simulations of flows in periodic domains. One of the essential characteristics occurring in the problems is the formation of small boundary layers around the arched borders, whose treatment was based on adaptive mesh refinement. It was observed that the periodic structure of the flow in the two geometries considered is fairly distributed as expected.

Regarding the periodic connection of the elements, it is verified that the matricial modification to establish it disturbs the global structure of the system. Although this numerical strategy is advantageous because of "deluding" the node indexing to enforce the periodicity without needing a spatial change, this process requires caution as to overlapping of boundary conditions at corner points and has caught the author's attention to improvements.

The model of decomposition of the pressure replaces the original pressure of the system and is fundamental to drive the fluid motion along the domain, thus working as a mass flow injector and the bringing up plausible results. Different situations have been studied to assure its applicability to the most general range of fluid flows. Henceforth, numerical models mingling further boundary conditions are foreseen to boost the source code now proposed, also including two-phase flow dynamics.

6. ACKNOWLEDGEMENTS

The authors would like to thank CAPES and the program Science Without Borders for the sponsoring of this work.

7. REFERENCES

Beale, S., 2007. "Use of streamwise periodic boundary conditions for problems in heat and mass transfer". *Journal of Heat Transfer*, Vol. 129, No. 4, pp. 601–605.

Lahbabi, A. and Chang, H.C., 1986. "Flow in periodically constricted tubes: transition to inertial and nonsteady flows". *Chemical Engineering Science*, Vol. 41, No. 10, pp. 2487–2505.

Mangiavacchi, N., Oliveira, G., Anjos, G. and Thome, J., 2013. "Numerical simulation of a periodic array of bubbles in a channel". *Mecánica Computacional*, Vol. XXXII, No. 21, pp. 1813–1824.

McGrath, D. and Pyati, V., 1996. "Periodic structure analysis using a hybrid finite element method". *Radio Science*, Vol. 31, No. 5, pp. 1173–1179.

Murthy, J. and Mathur, S., 1997. "Periodic flow and heat transfer using unstructured meshes". *International Journal for Numerical Methods in Fluids*, Vol. 25, No. 6, pp. 659–677.

Nonino, C. and Comini, G., 1998. "Finite-element analysis of convection problems in spatially periodic domains". *Numerical Heat Transfer, Part B*, Vol. 34, No. 4, pp. 361–378.

Patankar, S., Liu, C. and Sparrow, E., 1977. "Fully developed flow and heat transfer in ducts having streamwise-periodic variations of cross-sectional area". *Journal of Heat Transfer*, Vol. 99, pp. 180–186.

Reddy, J., 1993. *An Introduction to the Finite Element Method.* McGraw-Hill.

Segal, G., Vuik, K. and Kassels, K., 1994. "On the implementation of symmetric and antisymmetric periodic boundary conditions for incompressible flow". *International Journal for Numerical Methods in Fluids*, Vol. 18, No. 12, pp. 1153–1165.

Sukumar, N. and Pask, J., 2009. "Classical and enriched finite element formulations for bloch-periodic boundary conditions". *International Journal for Numerical Methods in Fluids*, Vol. 77, No. 8, pp. 1121–1138.

Taylor, G., 1923. "Lxxv. on the decay of vortices in a viscous fluid". *The London, Edinburgh, and Dublin Philosophical Magazine and Journal of Science*, Vol. 46, No. 274, pp. 671–674.

Tyrus, J.M., Gosz, M. and DeSantiago, E., 2007. "Periodic structure analysis using a hybrid finite element method". *International Journal of Solids and Structures*, Vol. 44, No. 9, pp. 2972–2989.

Yazdchi, K., Srivastava, S. and Luding, S., 2011. "Microstructural effects on the permeability of periodic fibrous porous media". *International Journal of Multiphase Flow*, Vol. 37, No. 8, pp. 956–966.

Zenklusen, A., Kenjereš, S. and von Rohr, P., 2014. "Vortex shedding in a highly porous structure". *Chemical Engineering Science*, Vol. 106, pp. 253–263.

8. RESPONSIBILITY NOTICE

The authors are the only responsible for the printed material included in this paper.